

Highly selective separation of toluene/methylcyclohexane based on pagoda[5]arene nonporous adaptive crystals

Zhongwen Liu,^{a,‡} Ming Li^{*a,‡}, Shuai Fang,^a Li Shao,^c Bin Hua^{*a,b} and Feihe Huang^{*a,b}

^a*Stoddart Institute of Molecular Science, Department of Chemistry, Zhejiang University,
Hangzhou 310058, P. R. China; Fax and Tel: +86-571-8795-3189*

^b*Zhejiang-Israel Joint Laboratory of Self-Assembling Functional Materials, ZJU-Hangzhou
Global Scientific and Technological Innovation Center, Zhejiang University, Hangzhou
311215, P. R. China*

^c*Department of Materials Science and Engineering, Zhejiang Sci-Tech University, Hangzhou
310018, P. R. China*

Email addresses: mingzhelee@zju.edu.cn; huabin@zju.edu.cn; fhuang@zju.edu.cn

Electronic Supplementary Information

1. <i>Materials and methods</i>	S2
2. <i>Synthesis of host P5</i>	S4
3. <i>Investigation of host–guest complexation behavior in solution</i>	S5
4. <i>Studies of selective adsorption behavior of P5 solid</i>	S10
5. <i>X-ray crystal data of P5⊃2Tol</i>	S20
6. <i>References</i>	S21

1. Materials and methods

Materials

All reagents including guest compounds were commercially available and used as supplied without further purification. Solvents were either employed as purchased or dried according to procedures described in the literature. Compound **P5** was prepared according to a published procedure.^{S1}

Methods

¹H NMR: NMR spectra were recorded with a Bruker Avance DMX 600 spectrophotometer or a Bruker Avance DMX 400 spectrophotometer using the deuterated solvent as the lock and the residual solvent or TMS as the internal reference.

Thermogravimetric analysis: TGA was carried out using a Q5000IR analyzer (TA Instruments) with an automated vertical overhead thermo balance. The samples were heated at 10 °C/min using N₂ as the protective gas.

X-ray powder diffraction: PXRD data were measured on a SmartLab diffractometer with fixed divergence slits and a D/tex Ultra 250 detector at room temperature. The diffractometer was configured in parafocusing Bragg-Brentano geometry. Data was collected over a 2θ range of 5° to 45° with a step size of 0.02° and a scan rate of 5°/min using a Cu K_{α} radiation at a powder of 40 kV and 180 mA. Cu K_{β} radiation was removed using a divergent beam Ni filter.

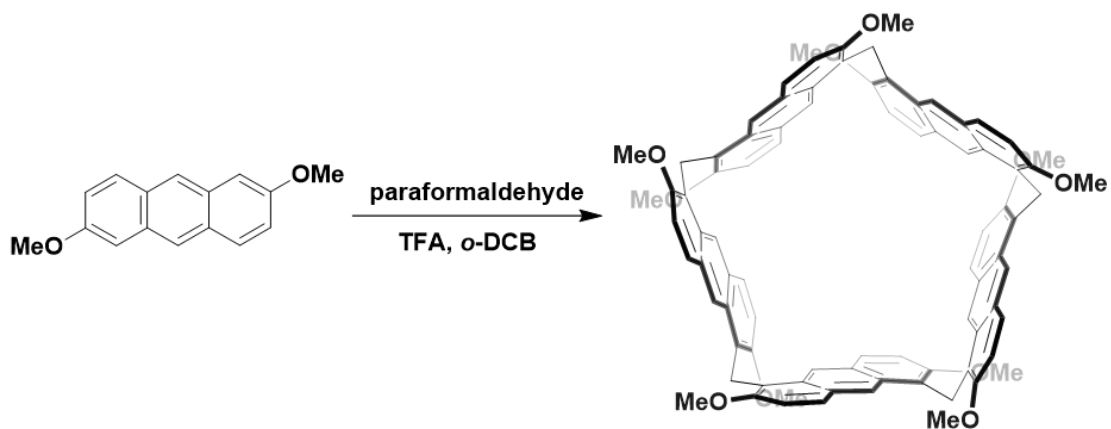
Gas chromatographic analysis: GC analysis measurements were carried out using an Agilent 7890B instrument configured with an FID detector and a HP-chiral β column (30 m \times 0.32 mm \times 0.25 μ m). Samples were analyzed using headspace injections and were performed by incubating the sample at 85 °C for 30 min followed by sampling 1.00 mL of the headspace. The total volume of the container is 10 mL; the mass of the solid in the container is about 10 mg; the total volume of the headspace is 1 mL.

Independent gradient model calculation: All-electron DFT calculations have been carried out by the latest version of ORCA quantum chemistry software

(Version 5.0.4).^{S2} The BLYP functional and the def2-SVP basis set^{S3} were adopted for geometry optimization calculation, and the optimal geometry for the complex was determined. The calculated complex structure was built from the single crystal structure of the complex. The positions of the H atoms were optimized, and the other atoms keep their positions unchanged. The nature of noncovalent interactions were studied by using the Independent Gradient Model (IGM) method^{S4} through Multiwfn software.^{S5} The visualization of IGM was rendered by VMD software.^{S6}

Single crystal X-ray diffraction: SCXRD data were collected on a Bruker D8 VENTURECMOS X-ray diffractometer with graphite monochromatic Mo- K_{α} radiation ($\lambda = 0.71073 \text{ \AA}$).

2. Synthesis of host **P5**



Scheme S1. Synthetic route to **P5**.

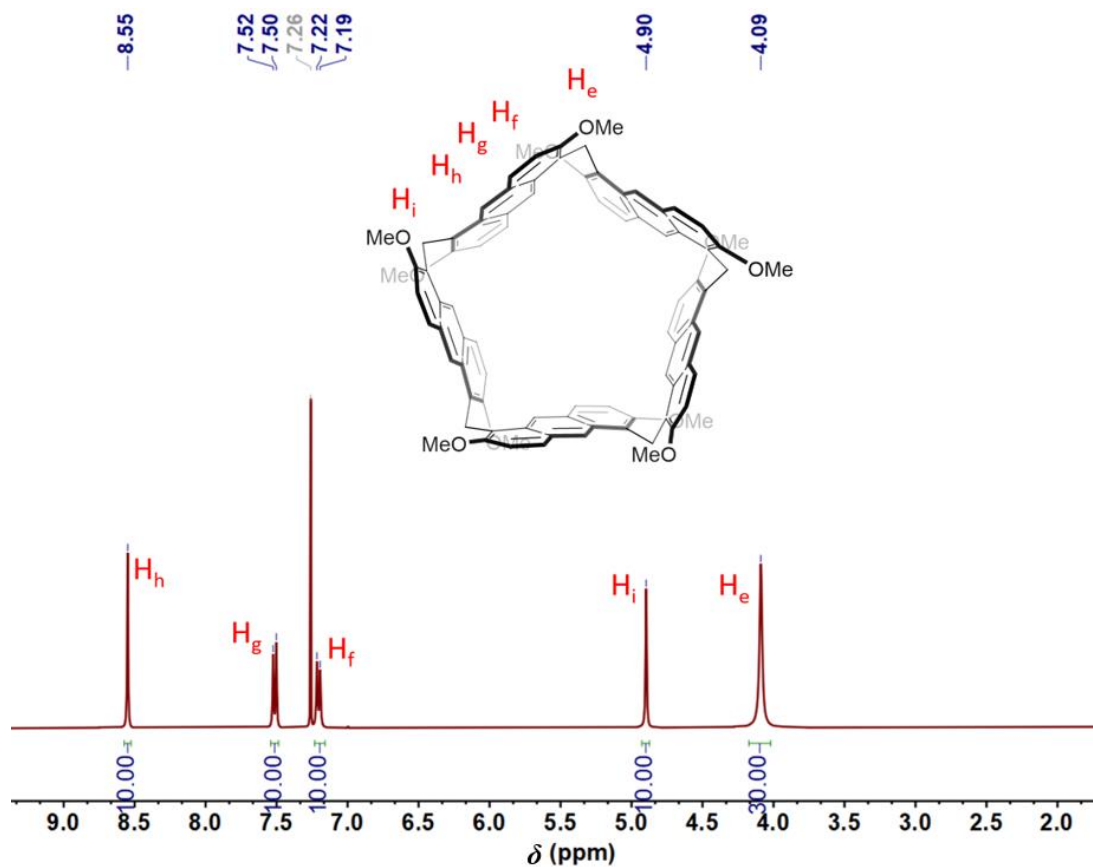


Fig. S1 ^1H NMR spectrum (400 MHz, CDCl_3 , room temperature) of **P5**.

3. Investigation of host-guest complexation behavior in solution

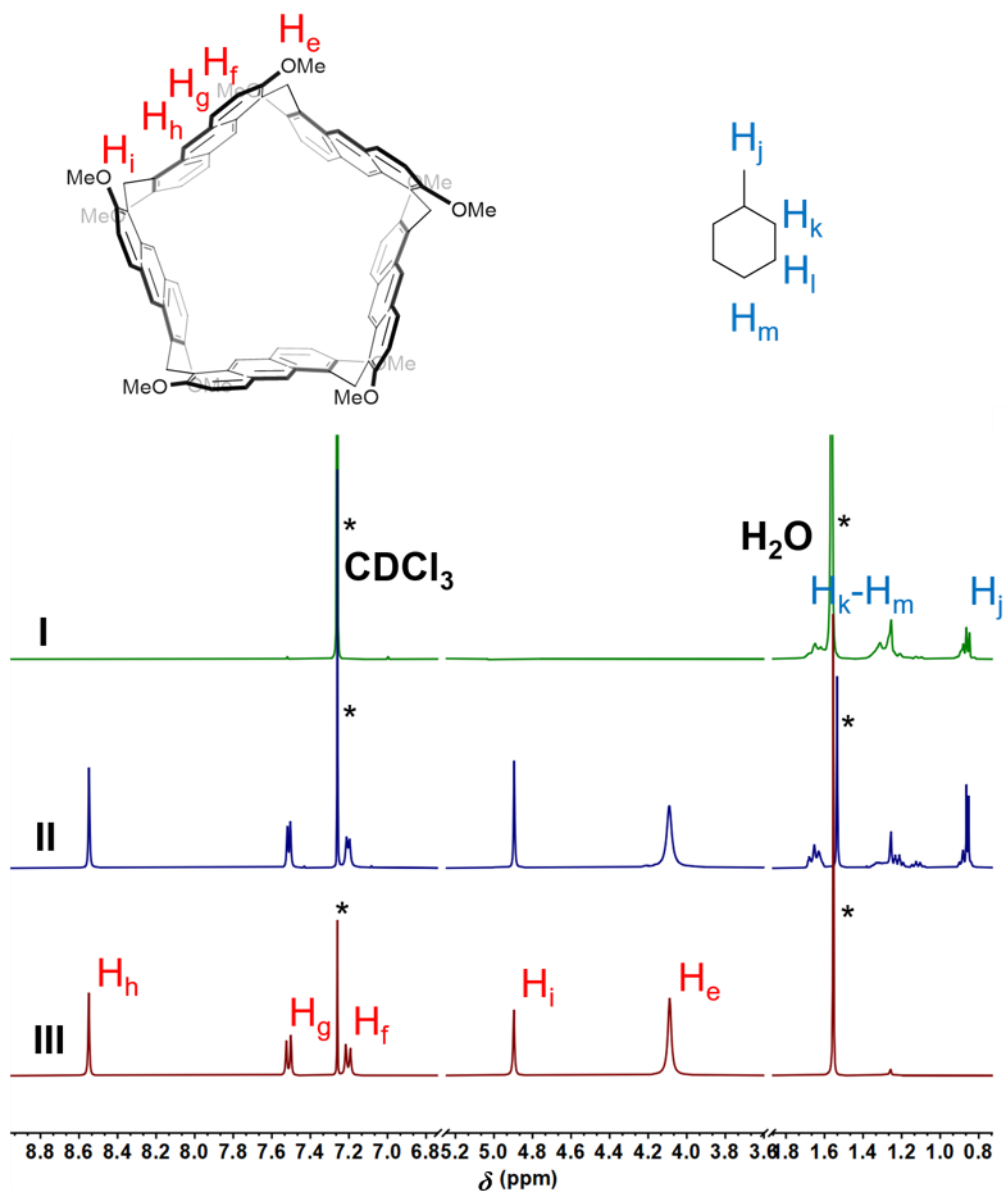


Fig. S2 Partial ^1H NMR spectra (400 MHz, CDCl_3 , room temperature): (I) **MCH**; (II) 3.00 mM **P5** and 6.00 mM **MCH**; (III) **P5**. Peaks marked with * are due to residual solvents.

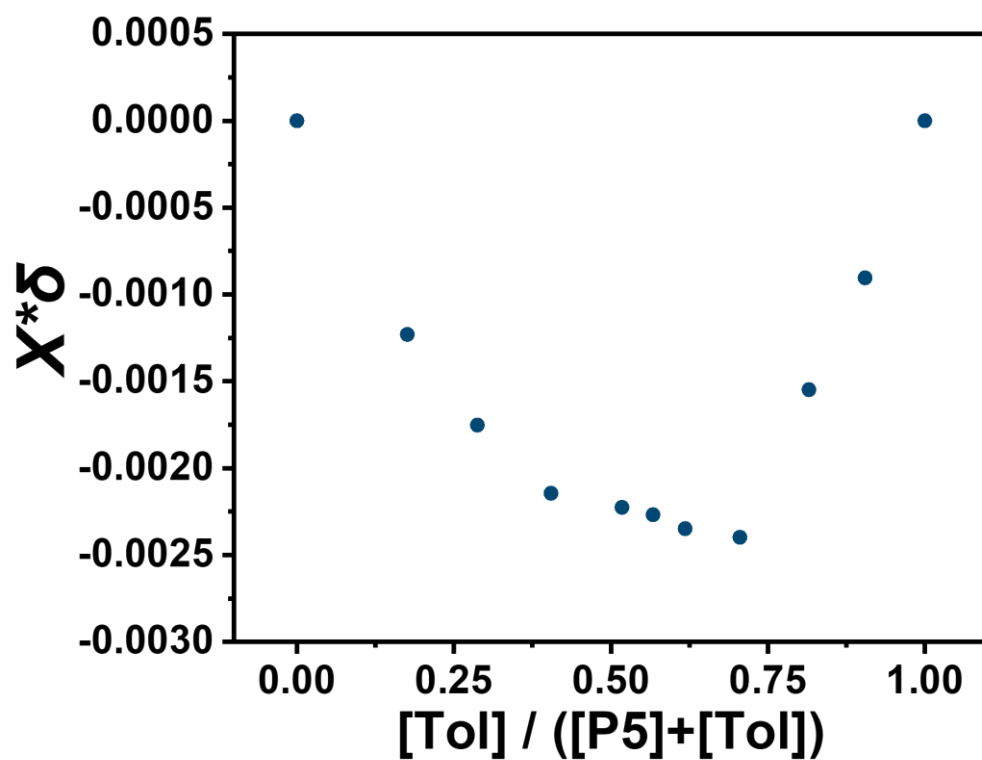


Fig. S3 Based on ^1H NMR spectroscopic results, a Job Plot was created to study the binding stoichiometry between **P5** and **Tol**. The total concentration of **[P5]** and **[Tol]** was set at 1.00 mM. The minimum peak is corresponding to the value of 0.67 ($[\text{Tol}]/([\text{P5}]+[\text{Tol}])$) for the mole fraction X of the guest **Tol**, a finding consistent with a 1:2 (**P5:Tol**) binding stoichiometry.

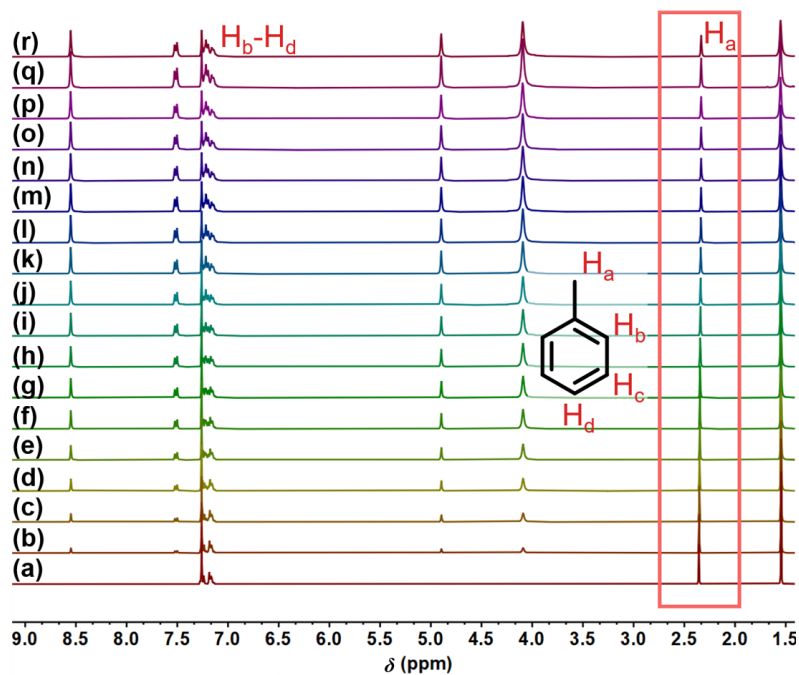


Fig. S4 Partial ^1H NMR spectra (400 MHz, CDCl_3 , room temperature) of **Tol** at a constant concentration of 5.00 mM upon gradually addition of **P5**. The concentrations of **P5** in solution: (a) 0.00 mM; (b) 0.48 mM; (c) 0.91 mM; (d) 1.31 mM; (e) 1.67 mM; (f) 2.00 mM; (g) 2.31 mM; (h) 2.60 mM; (i) 2.86 mM; (j) 3.27 mM; (k) 3.68 mM; (l) 4.03 mM; (m) 4.39 mM; (n) 4.71 mM; (o) 5.00 mM; (p) 5.26 mM; (q) 5.56 mM; (r) 5.81 mM.

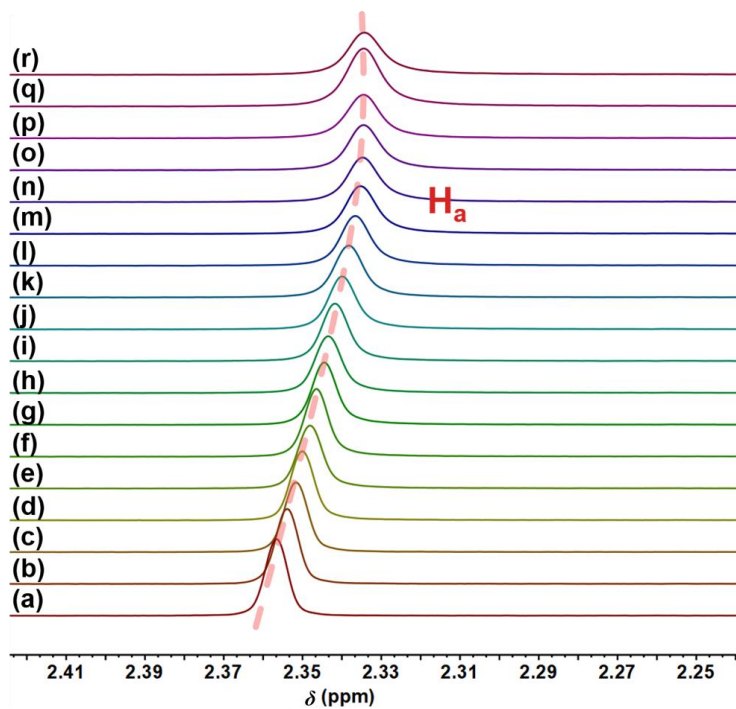


Fig. S5 The marked region (from 2.0 ppm to 2.5 ppm) of Fig S4. The trajectory of the observed chemical shift variations is illustrated by the red dashed line.

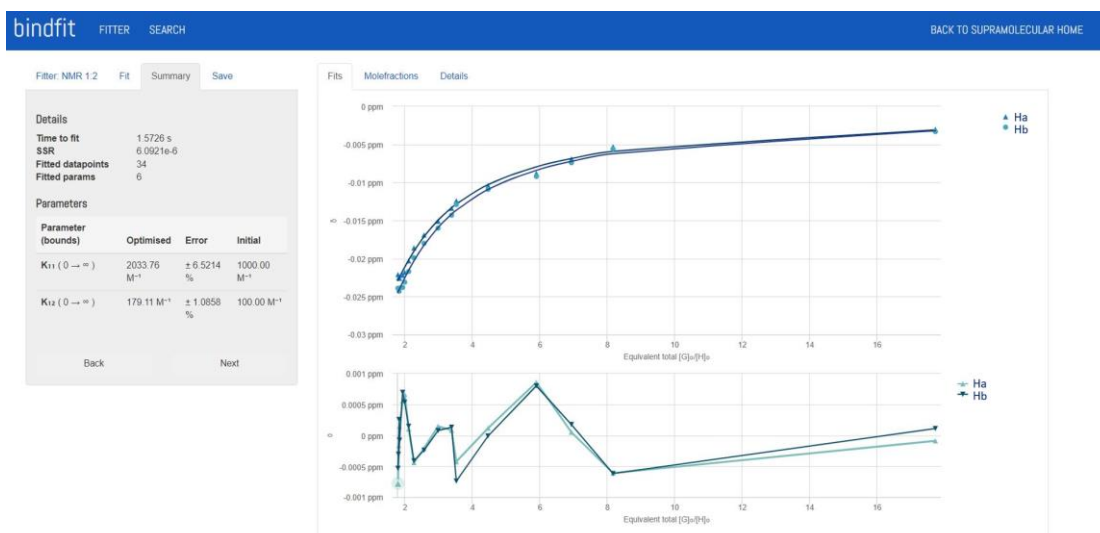


Fig. S6 A graph was plotted to illustrate the resonance upfield shifts of H_a and H_b of **Tol** with respect to the molar ratio of [Tol]/[P5]. The data were fitted to a 1:2 binding model, yielding $K_{a1} = (2.03 \pm 0.13) \times 10^3 \text{ M}^{-1}$ and $K_{a2} = (1.79 \pm 0.02) \times 10^2 \text{ M}^{-1}$. The solid lines on the graph were obtained through non-linear curve-fitting using the web applet available at www.supramolecular.org.

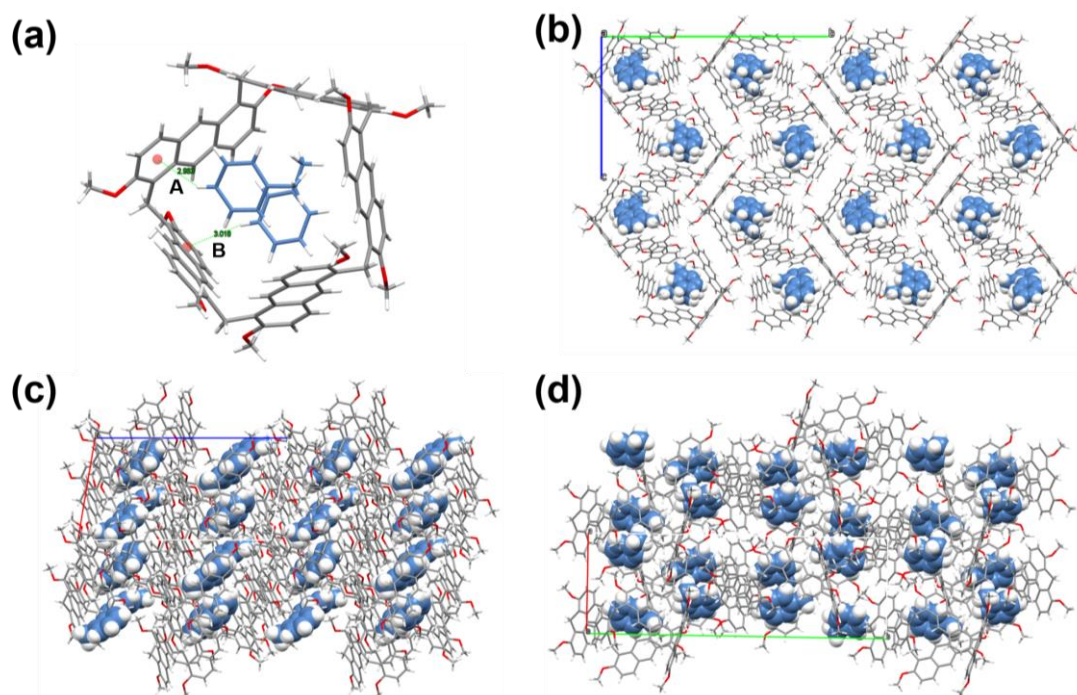


Fig. S7 (a) Single crystal structure of **P5⊃2Tol**. C–H···π distances (Å) and C–H···π angles (degrees) of hydrogen bonds: **A**: 2.96, 147.47; **B**: 3.02, 166.70. Different views of the single crystal structure of **P5⊃2Tol**: (b) along the *a*-axis; (c) along the *b*-axis; (d) along the *c*-axis. The green dotted lines represent the C–H···π interactions. The solvent molecules have been removed for clarity.

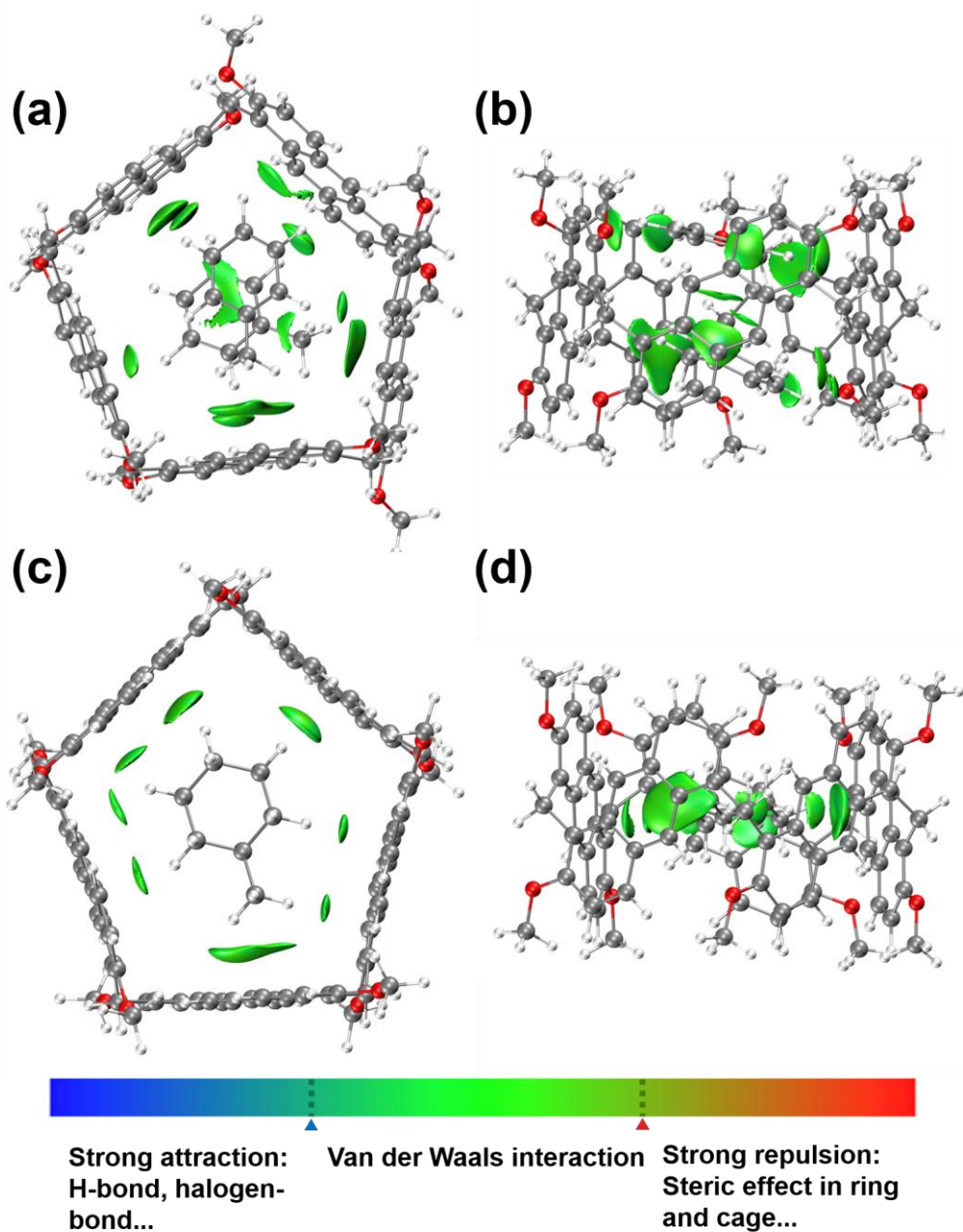


Fig. S8 The noncovalent interaction graphs of **P5⊃2Tol** and **MCH-loaded P5** obtained through the IGM calculation: (a) top view of **P5⊃2Tol**; (b) side view of **P5⊃2Tol**; (c) top view of **MCH-loaded P5**; (d) side view of **MCH-loaded P5**.

4. Studies of selective adsorption behavior of **P5** solid

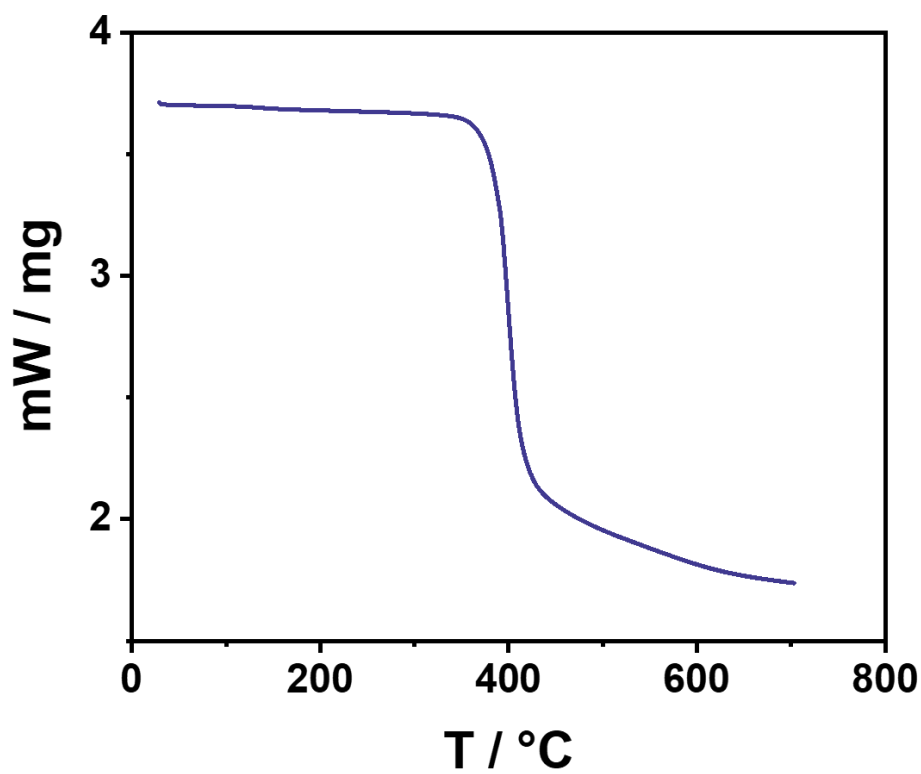


Fig. S9 Thermogravimetric analysis of guest-free **P5**.

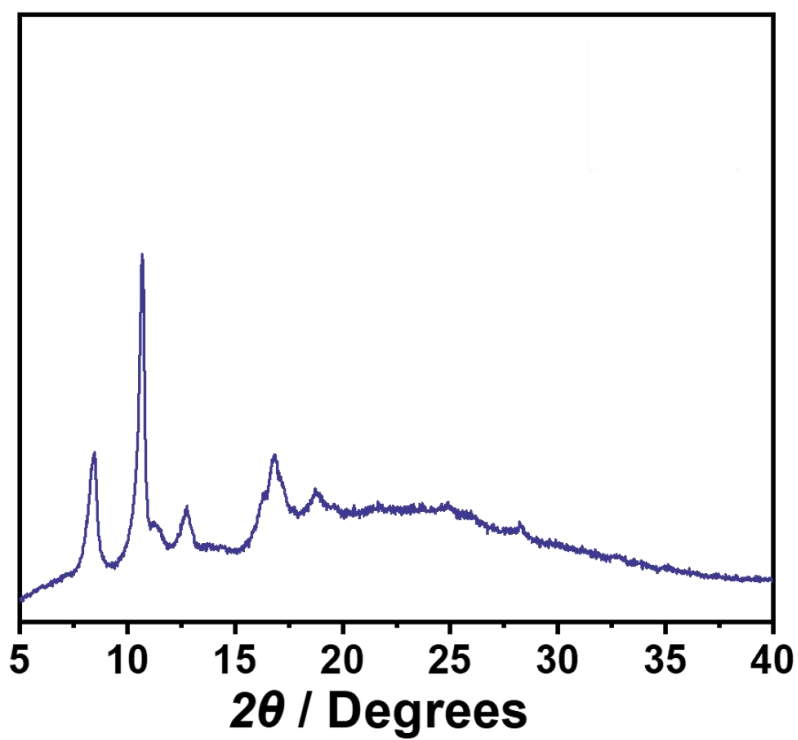


Fig. S10 Powder X-ray diffraction pattern of guest-free **P5**.

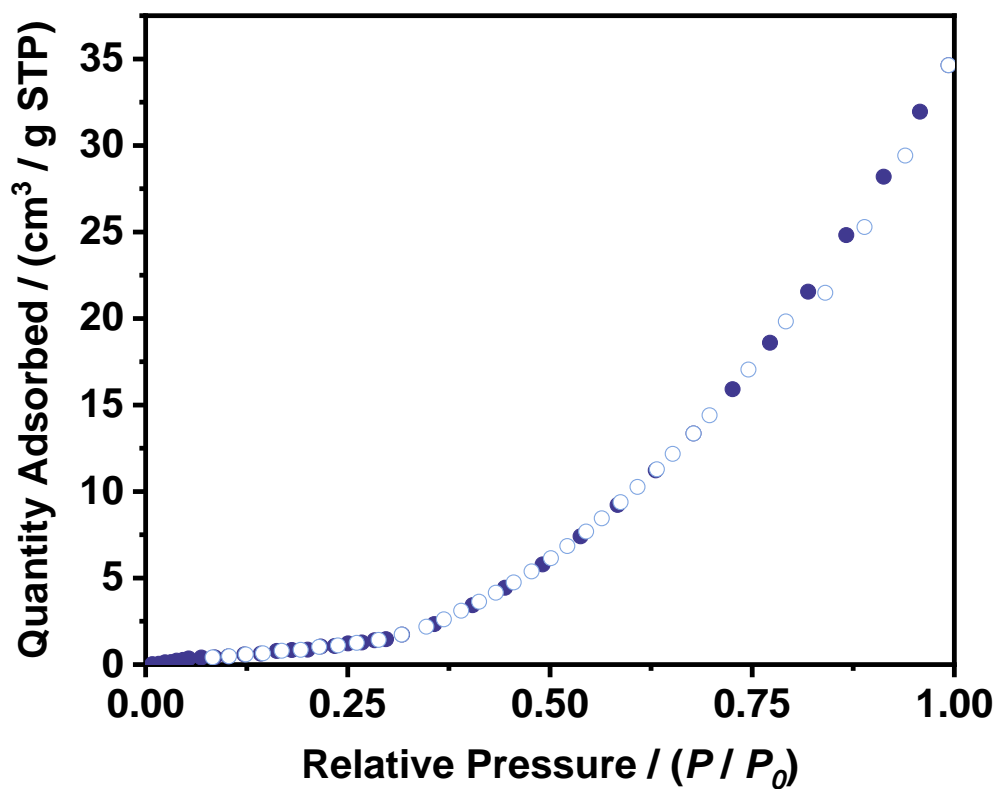


Fig. S11 N₂ adsorption isotherm of guest-free **P5**. The BET surface area value is 2.98 m² g⁻¹.

Adsorption, solid symbols; desorption, open symbols.

Method: For each solid-vapor adsorption experiment, an open 5 mL vial containing 3 mg of the guest-free **P5** adsorbent was placed in a sealed 20 mL vial containing 1 mL of **Tol**, **MCH**, or a **Tol/MCH** mixture (v:v = 1:1).

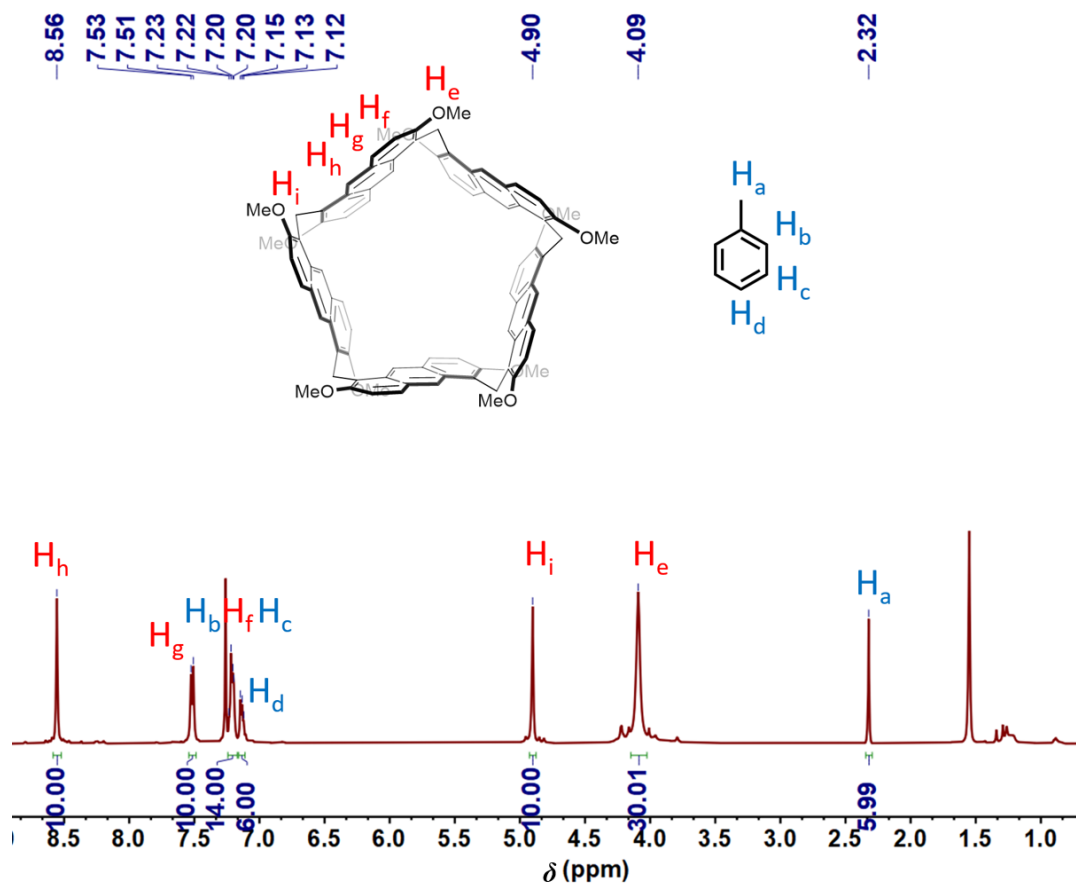


Fig. S12 ¹H NMR spectrum (400 MHz, CDCl₃, room temperature) of guest-free **P5** after being exposed to **Tol** vapor for 24 h. Based on the integrated areas under these NMR peaks, approximate 2.0 equivalents of **Tol** molecules were absorbed per **P5** molecule.

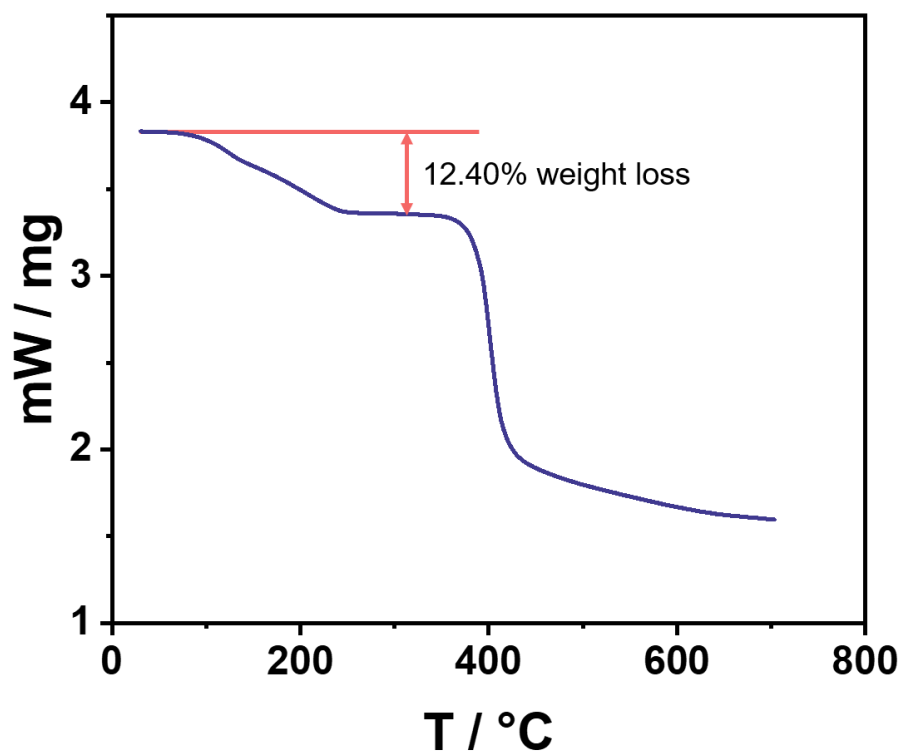


Fig. S13 Thermogravimetric analysis of guest-free **P5** after being exposed to **Tol** vapor for 24 h. The weight loss below 250 °C corresponds to approximately 2.0 equivalents of **Tol** molecules per **P5** molecule.

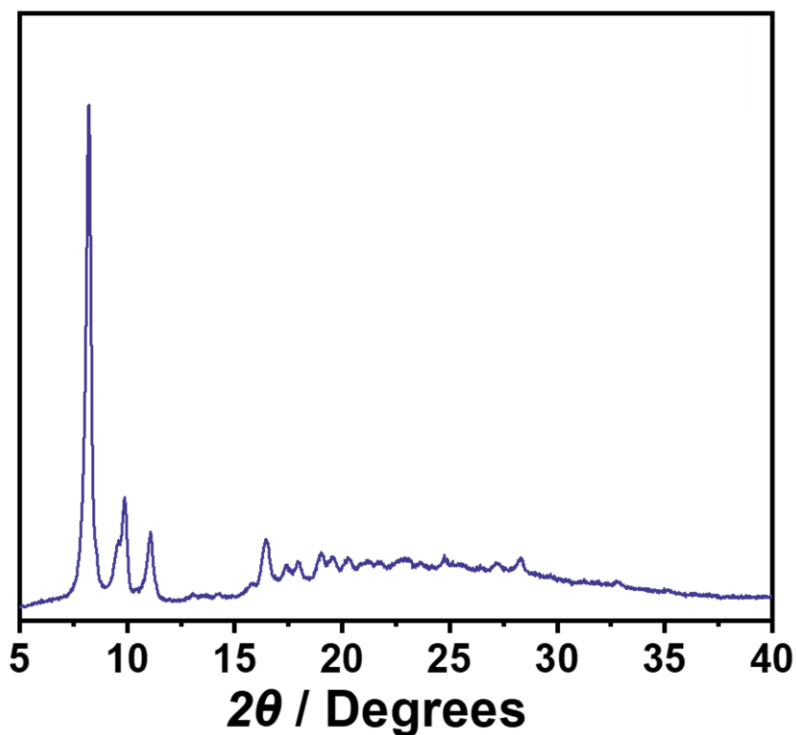


Fig. S14 Powder X-ray diffraction of guest-free **P5** after being exposed to **Tol** vapor for 24 h.

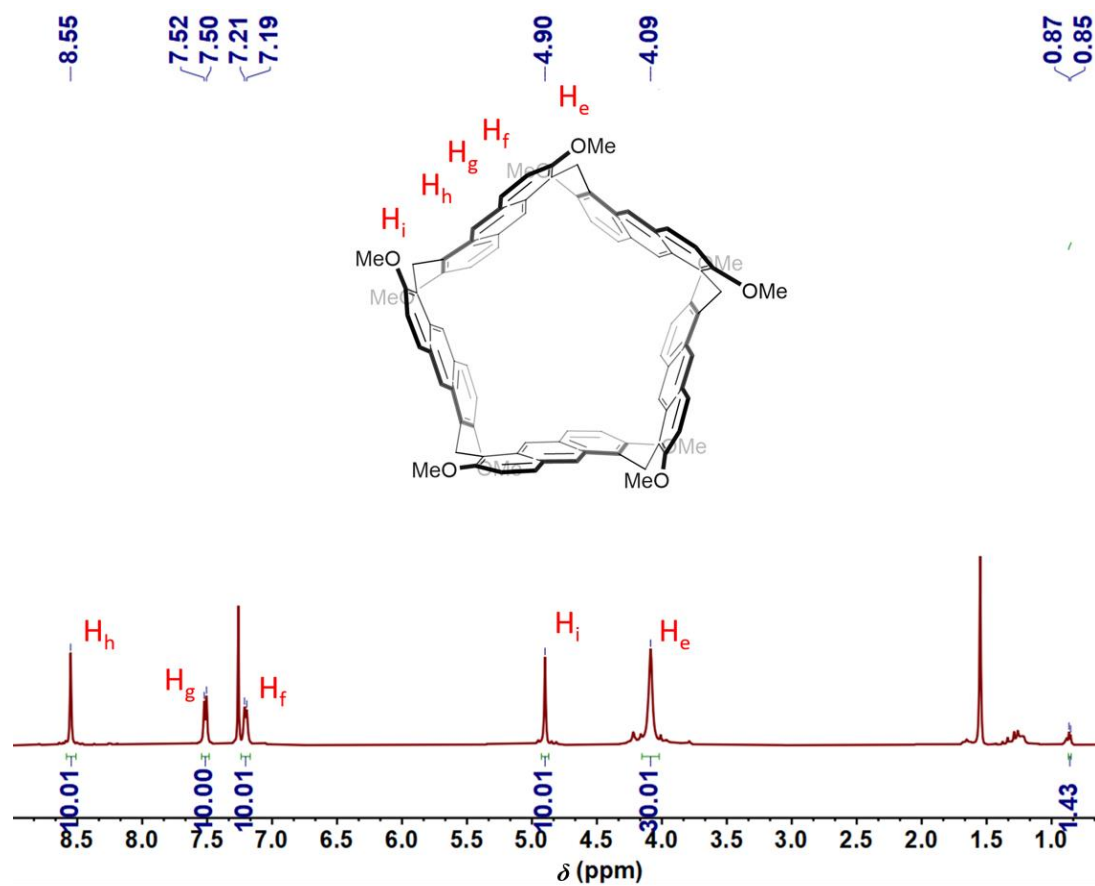


Fig. S15 ^1H NMR spectrum (400 MHz, CDCl_3 , room temperature) of guest-free **P5** after being exposed to **MCH** vapor for 24 h. The integrated areas under these peaks show no significant adsorption of **P5** for **MCH**.

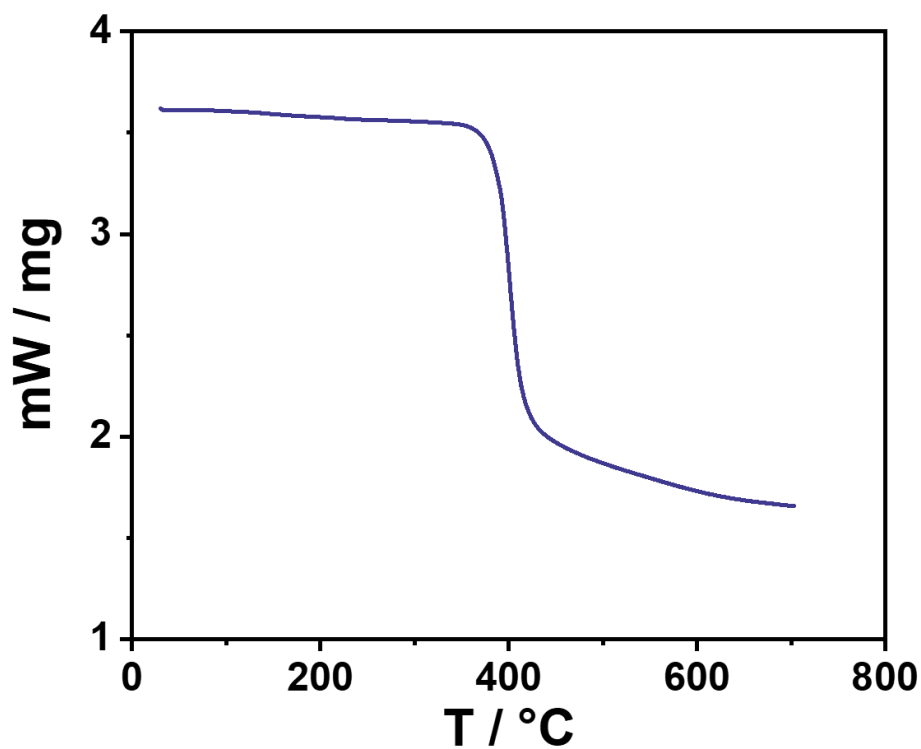


Fig. S16 Thermogravimetric analysis of guest-free **P5** after being exposed to **MCH** vapor for 24 h. No significant weight loss of **P5** before 350 °C was observed after adsorption of **MCH** vapor.

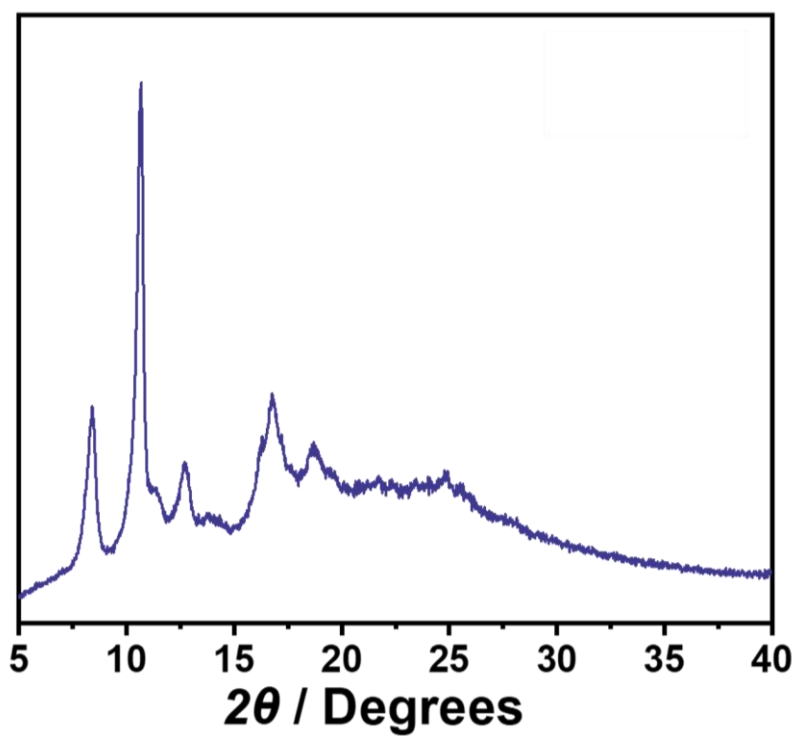


Fig. S17 Powder X-ray diffraction of guest-free **P5** after being exposed to **MCH** vapor for 24 h.

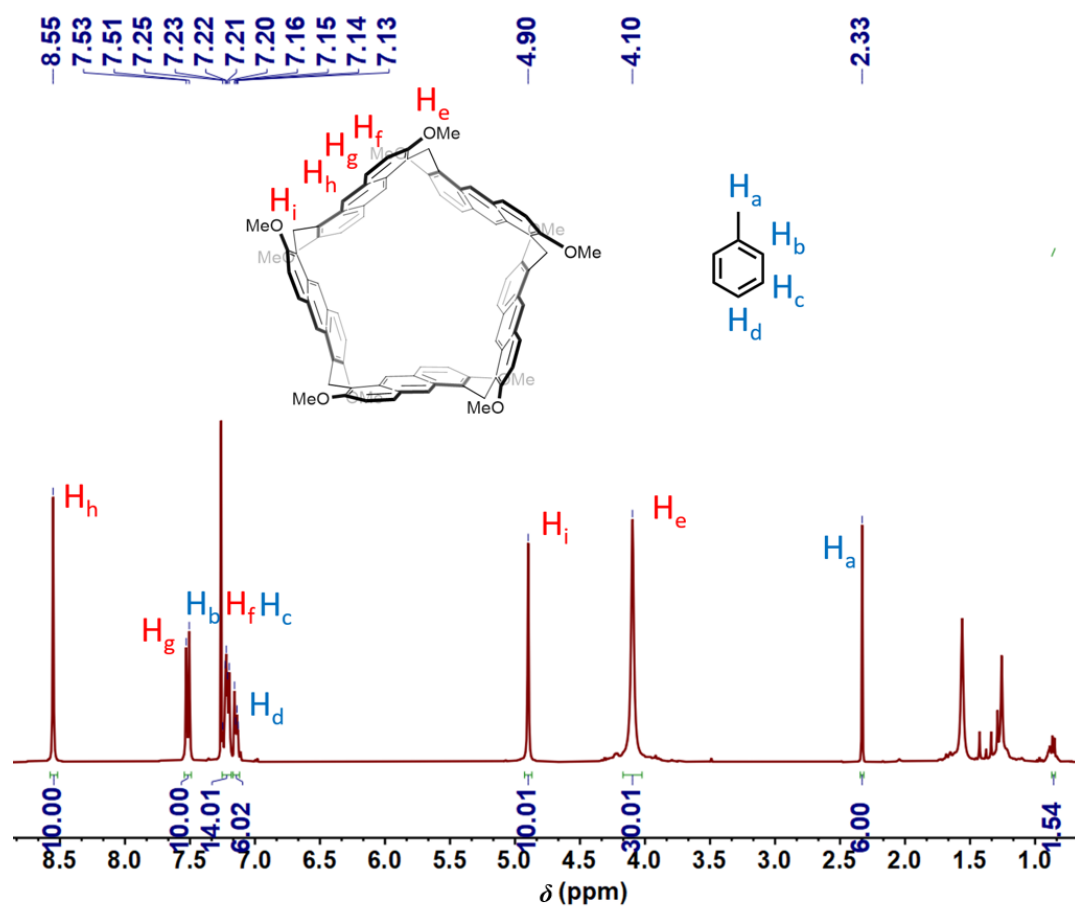


Fig. S18 ¹H NMR spectrum (400 MHz, CDCl₃, room temperature) of guest-free **P5** after being exposed to equivolume mixture vapor of **Tol** and **MCH** for 24 h. The integrated areas under these peaks correspond to approximate 2.0 equivalents of **Tol** and a trace amount of **MCH** per **P5** molecule.

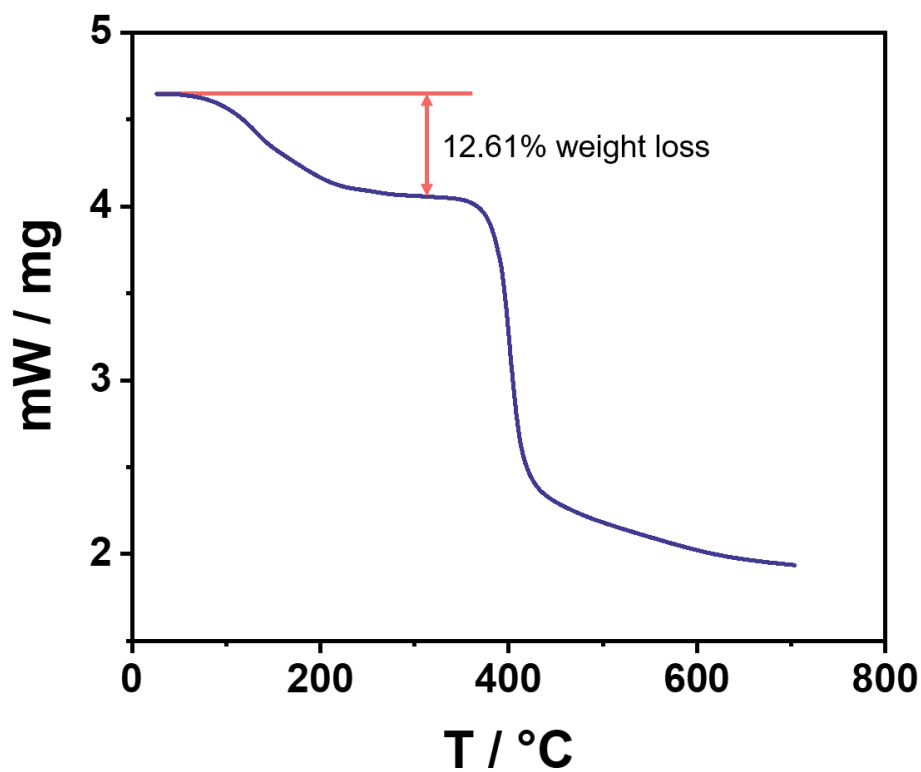


Fig. S19 Thermogravimetric analysis of guest-free **P5** after being exposed to equivolume mixture vapor of **Tol** and **MCH** for 24 h. The weight loss below 250 °C corresponds to approximately 2.0 equivalents of **Tol** molecules per **P5** molecule.

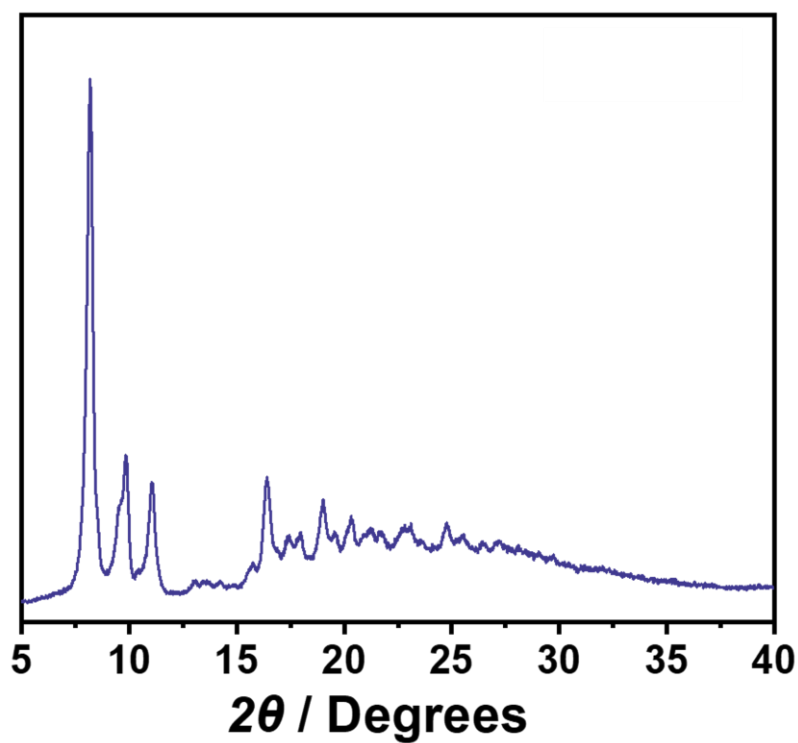


Fig. S20 Powder X-ray diffraction of guest-free **P5** after being exposed to equivolume mixture vapor of **Tol** and **MCH** for 24 h.

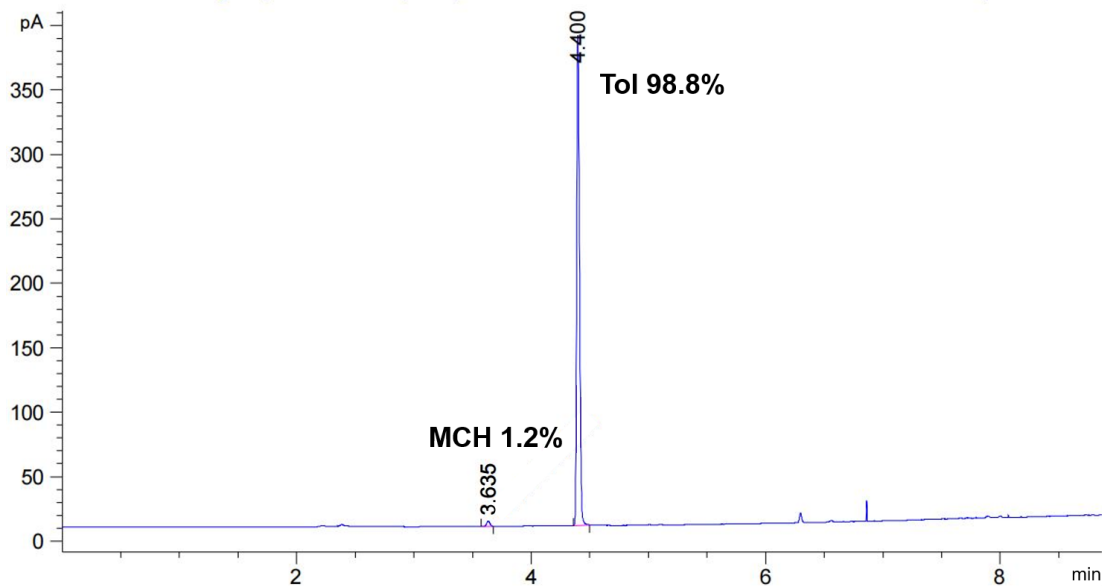


Fig. S21 Gas chromatography of guest-free **P5** after being exposed to equivolume mixture vapor of **Tol** and **MCH** for 24 h.

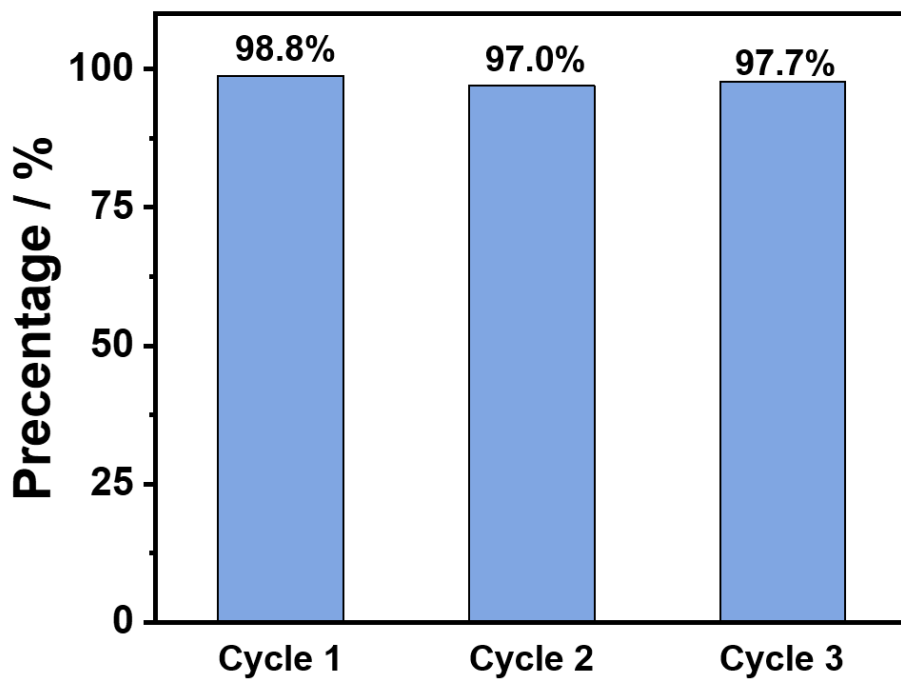


Fig. S22 The selectivity of **Tol** uptake by **P5 α** over three cycles.

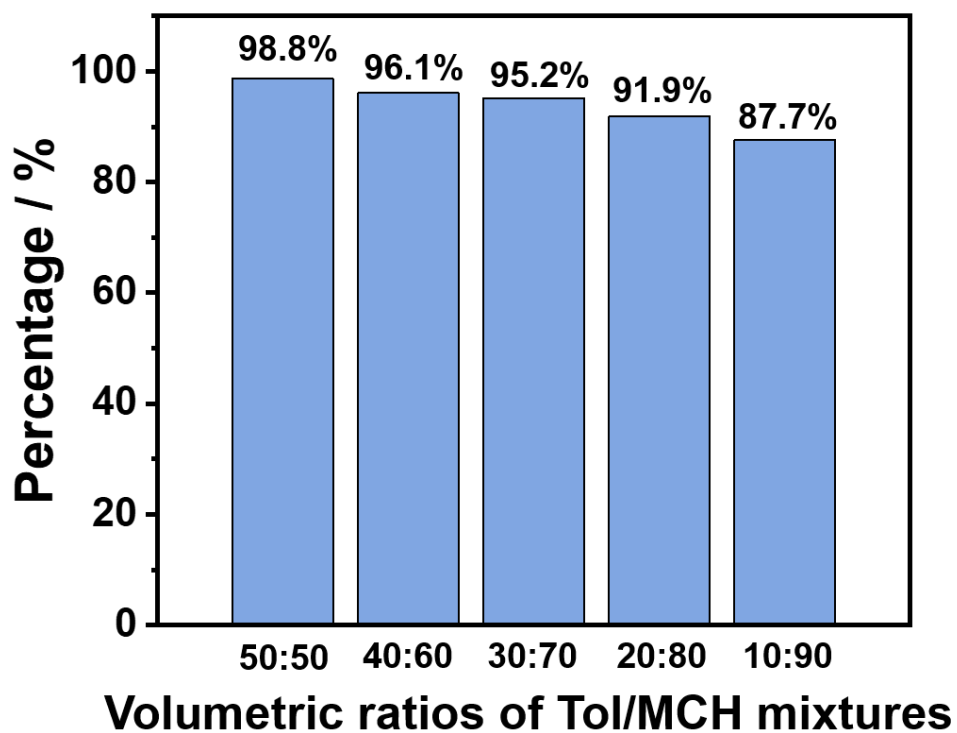


Fig. S23 The relative amounts of **Tol** adsorbed in **P5 α** at different volumetric ratios of **Tol/MCH** mixtures.

5. X-ray crystal data of **P5**⊃**2Tol**

Yellow crystals were obtained by slow diffusion of MeOH into a mixed solution containing **P5**, **Tol** and CHCl₃. In the single crystal structure of **P5**⊃**2Tol**, the molar ratio of **P5** and **Tol** in the resulting host–guest complex crystal structure was 1:2. CCDC number: 2289677.

Table S1. Experimental crystallographic data for the crystal of **P5**⊃**2Tol**.

Parameters	P5 ⊃ 2Tol
Formula	C ₁₀₀ H ₈₇ Cl ₃ O ₁₀
FW	1555.04
Temp. (K)	213.00
Crystal system	Monoclinic
Space group	<i>P2</i> ₁ / <i>n</i>
<i>a</i> (Å)	11.3466(4)
<i>b</i> (Å)	33.1889(10)
<i>c</i> (Å)	21.1629(8)
α (°)	90
β (°)	99.491(3)
γ (°)	90
Volume (Å ³)	7860.5(5)
<i>Z</i>	4
ρ_{calc} (g cm ⁻³)	1.314
<i>F</i> (000)	3272
Independent reflections	14915 [<i>R</i> _{int} = 0.1496]
Goodness-of-fit on <i>F</i> ²	1.029
Final <i>R</i> indexes [<i>I</i> ≥ 2σ(<i>I</i>)]	<i>R</i> ₁ = 0.1054, <i>wR</i> ₂ = 0.2794
Final <i>R</i> indexes [all data]	<i>R</i> ₁ = 0.2275, <i>wR</i> ₂ = 0.3649
Largest diff. peak/hole (e Å ⁻³)	0.753/-0.685

6. References

- S1. X. Han, Q. Zong, Y. Han and C. Chen, Pagoda[5]arene with large and rigid cavity for the formation of 1:2 host–guest complexes and acid/base-responsive crystalline vapo-chromic properties, *CCS Chem.*, 2022, **4**, 318–330.
- S2. F. Neese, Software update: The ORCA program system—Version 5.0, *WIREs Comput Mol Sci.*, 2022, **12**, e1606.
- S3. F. Weigend and R. Ahlrichs, Balanced basis sets of split valence, triple zeta valence and quadruple zeta valence quality for H to Rn: Design and assessment of accuracy, *Phys. Chem. Chem. Phys.*, 2005, **7**, 3297–3305.
- S4. T. Lu and Q. Chen, Independent gradient model based on Hirshfeld partition: A new method for visual study of interactions in chemical systems, *J. Comput. Chem.*, 2022, **43**, 539.
- S5. T. Lu and F. Chen, Multiwfn: A multifunctional wavefunction analyzer, *J. Comput. Chem.*, 2012, **33**, 580–592.
- S6. W. Humphrey, A. Dalke and K. Schulten, VMD: Visual molecular dynamics, *J. Molec. Graphics*, 1996, **14**, 33–38.